

Central European Journal of Chemistry

Corrosion depth profiles of nitrided titanium alloy in acidified sulphate solution

Research Article

Karina Jagielska-Wiaderek^{1*}, Henryk Bala¹, Tadeusz Wierzchon²

¹Division of Chemistry, Faculty of Materials Engineering and Applied Physics, Czestochowa University of Technology, 42-200 Czestochowa, Poland

²Faculty of Materials Science and Engineering, Warsaw University of Technology, PL-02 507 Warszawa, Poland

Received 20 March 2013; Accepted 15 July 2013

Abstract: Thick ($400 \, \mu m$) glow-discharge nitrided layers, $TiN + Ti_2N + \alpha Ti(N)$ type, have been produced on the Ti-1Al-1Mn titanium alloy. Using a progressive thinning method, the polarization characteristics at different depths of nitrided layers have been measured. From the plots of obtained potentiodynamic polarization curves the depth profiles of characteristic anodic and cathodic currents (at potentials corresponding to (a) hydride formation, (b) hydrogen evolution, (c) primary passivation, (d) oxygen evolution and (e) secondary passivation) as well as polarization resistance have been determined in 0.5 M Na_2SO_4 solution acidified to pH = 2. The anomalously high slope of the polarization curves in the cathodic region has been ascribed to the formation of titanium hydride. It has been shown that outer nitrided layers (up to $25 \, \mu m$) exhibit excellent acid corrosion resistance owing to strong inhibition of the anodic process by TiN phase. Corrosion resistance of deeper situated layers gradually decreases and at depths of $250-370 \, \mu m$ the corrosion process is accelerated by presence of TiO_2 precipitations. Nitrided layers, unlike the alloy core, allow oxygen evolution on the oxy-nitrided surface at potential of $+1.6 \, V$ and at more positive potentials gradual transformation of the surfacial film into TiO_2 takes place. Secondary passivation on nitrided titanium is less efficient than that in the absence of Ti-N species.

Keywords: Titanium • Nitriding • Electrochemical corrosion • Depth-profile © Versita Sp. z o.o.

1. Introduction

Nitriding of titanium and its alloys produces surface layers due to the presence of titanium nitrides $TiN+Ti_2N$ and solid solution of nitrogen $\alpha Ti(N)$ that exhibit both metallic (Ti-Ti) and covalent (Ti-N) bonding characteristics. Properties arising from the metallic bonding characteristics are the electrical/heat- conductivity and metallic reflectance and properties resulting from the covalent bonding are high melting point, extreme hardness and brittleness, and excellent thermal, corrosion and erosion resistance [1-3]. These properties of TiN have been frequently exploited as protective and decorative coatings on titanium and many other substrates [1-5]. Additionally, TiN passivates in human fluids and shows satisfactory intrinsic

biocompatibility and hemocompatibility, thus it has been successfully applied as surface layers and electrical interconnects in orthopedic prostheses, cardiac valves and other biomedical devices [3,6,7]. Classification of contemporary titanium nitriding methods include ionbeam, plasma, laser and gas-nitriding [8]. Nitriding processes of Ti (700 - 1000°C, 2-15 hours) cause formation of a compound layer of TiN (hardness 2000-3000 HV) on top and Ti₂N (1200-1500 HV) beneath [8,9] (the initial hardness of Ti and its alloys varies between 200 and 400 HV depending on the material chemical composition). A simplified physical model of the kinetics of formation and growth of surface nitride layers on titanium has been presented by Malinov *et al.* [8,10]. The model shows that the nitrided layer consists of TiN and

^{*} E-mail: karina@wip.pcz.pl

 ${\rm Ti_2N}$ outer compound layers and the thick diffusion zone (interstitial solution of nitrogen in the hcp α -Ti phase). The thickness of obtained compound layers on Ti varies from 2 - 15 μ m (but for some of Ti alloys even up to 50 μ m) [8,11,12].

Titanium possesses excellent corrosion resistance in many environments [13-17]: it passivates spontaneously in the presence of oxygen and in water with formation of thin (<10 nm) surface oxide film of TiO, Ti₂O₃ and TiO₃ [18,19]. The oxide film is resistant to pitting- and crevice corrosion in the presence of halide ions [17]. Titanium undergoes active dissolution in strong acidic media (e.g. H₂SO₄, HCl, or, particularly, HF) with formation of adsorbed TiOH intermediates [15] and then Ti2+, Ti3+ and TiO₂²⁺ ions [13,14,18-21]. In strong acid solutions the active dissolution of Ti takes place at potentials of -0.7 to -0.1 V [13,20] and it seems likely that the process is controlled by the stage of titanium hydride transformation to adsorbed state [15,20]. According to Shcherbakov and Kasatkina [20], until the passivation of titanium begins the anodic dissolution rate linearly depends on electrode potential, i.e., titanium active dissolution process does not obey simple kinetics of electrode processes (no Tafel dependence in the active dissolution region).

Titanium dioxide exhibits unusual biocompatibility properties and cell integration which makes TiO₂-deposited titanium alloys excellent implant material for orthopedic and dental applications as well as metallic material for vascular stents [12, 2-26].

The kinetics of water reduction process on Ti surface is also very complicated and does not fulfill generally accepted mechanisms for cathodic hydrogen evolution. A strong hydrogen affinity to titanium [6,7,16,19] implies its specific adsorption and formation of hydride layers in the cathodic region [15,20]. The thickness of hydride layers increases proportionally with time. For example, according to Videm et al. [7] for pH = 0.8 to 5.3 and at 20 hours treatment with a cathodic current of 1 mA cm⁻² the thickness of TiH, layer was ca 13 µm [7]. The cathodic slopes for Ti are extraordinarily high: 0.3 - 0.4 V decade⁻¹ which is typical for hydride formation [7] and indicates an exceptional mechanism of cathodic process. Wilhelmsen and Grande [27] also observe that hydride formation suppresses the hydrogen evolution reaction on Ti. Rauscher and Lukacs [28] point out that titanium hydride may play a dominant role both in the hydrogen evolution reaction and in the self-dissolution process. Foroulis [29] also assumes hydrogen uptake (with hydride formation) by cathodically charged titanium and indicates anions that can inhibit or catalyze this process.

It is worth mentioning that alloying titanium with small amounts (0.1 - 0.5%) of platinum group metals (Pt, Pd, Rh, Ru or Ir) strongly decreases hydrogen evolution overpotential and transforms the alloy into passive state even in boiling $10\%\ H_2SO_4$ and HCl solutions [13]. Above mentioned additions inhibit titanium acid corrosion process by 1-2 orders of magnitude [13,30].

As it results from the cited papers, the TiN compound shows clearly manifested anti-corrosion properties. However, the structural features of the nitrided layers on titanium are not fully understood and therefore the depth profiles of corrosion properties for these layers needs to be understood. The transition area between compound- and diffusive layer probably consists of TiN and Ti₂N precipitates transformation in the Ti(N) solid solution and should induce galvanic effects. Passivation efficiency of the outer N-rich layers on titanium should depend on their phase structure and the mechanism of surface oxidation process should include reactions with nitrogen participation. Nitriding should also affect the titanium hydride/oxide transformation. As it results from many contemporary papers [22-26], TiO₂ exhibits many more advantages in view of biocompatibility compared to TiN. In order to enrich the outer nitrided layers with TiO, we modified the glow-discharge nitriding method by introducing air (about 1.0% by vol.) into the reaction chamber. This allows titanium nitride-TiN layers with TiO₂-rich zones, situated at the depths of 10-25 μm, to be obtained.

The present paper is aimed at the evaluation of parameters describing corrosion properties of nitrided layers on titanium on its cross section and effect of oxide inclusions. For this purpose we applied a technique named "progressive thinning" [31-33] which consists of step-by-step removal of 5-10 µm layers by precise grinding and measuring the polarization characteristics of the exposed surfaces.

2. Experimental procedure

The titanium alloy Ti-1Al-1Mn (chemical composition in mass %: 1.0 Al, 0.9Mn, 0.3Fe, 0.3Cr and 0.12 Si, balance Ti) was subjected to a glow discharge nitriding process at 900°C for 70 hours in a nitrogen (99.99%) atmosphere at the pressure in a working chamber equal to 3 mbar and then oxidizing in nitrogen and air (1.0%) mixture for 2.0 hours. The process temperature was controlled by a Rayomatic pyrometer and thermocouple [11,12]. The surface treatment parameters were selected to obtain a relatively thick surface layer (ca 400 μ m) that would have distinctly diversified properties on its

cross section, analogous to the other metallic materials reported previously [31-33].

The microstructure of the produced surface layers were examined using an optical Neophot 32 microscope. Metallographic specimens in cross-section layers were prepared by etching with an aqueous solution of $2\% \text{HNO}_3 + 2\% \text{HF}$. Microhardness (HV 0.05) was measured by the Vickers method. The phase composition of surface layers was examined using Philips PW 1830 diffractometer with CoK alpha radiation.

Potentiodynamic polarization tests were carried out in 0.5M sodium sulphate solution acidified with H₂SO, to pH = 2. Electrodes for the polarization testing had the form of rotating discs with the operating surface area of 0.196 cm². Prior to each potentiodynamic measurement parallel electrode layers of a thickness of 2 - 8 µm were taken off by polishing (waterproof emery paper, grade 1000) while proceeding from the surface into the depth of the alloy. After polishing, the electrodes were rinsed with distilled water, degreased with ethanol and, eventually, dried. The real thickness of the layers ground off was determined from the mass loss of the examined disc electrode in relation to its initial mass (before polishing) and established with an accuracy of ±0.02 mg (which corresponds to ±0.003 µm in the electrode thickness). The methodology described above has been applied in our previous papers [31-33] and named the progressive thinning method. The polarization measurements were carried out at a temperature of 25 ± 0.1°C with the disc rotation speed equal to 12 rps and with a potential scan rate of 10 mV s⁻¹, applying the potential scanning from $E_{\rm start}$ = -1.5 V up to the value of $E_{\rm end}$ = +3.0 V. The values of all the electrode potentials are expressed in this paper *versus* AgCI/Ag reference electrode, for which $E_{AqCI/Aq}^{eq}$ = 0.222 V.

3. Results and discussion

Sample microstructures of the top layer obtained as a result of glow-discharge nitriding of the tested Ti alloy are presented in Fig. 1. As shown in Fig. 1(A and B), the overall thickness of the modified layer is ca 370 $\mu m.$ As it has been established by XRD analysis in previous papers of our group [11,12], it consists of a few sublayers: TiN (up to 75 $\mu m),$ Ti_N (75 - 140 $\mu m)$ and solid solution of nitrogen in α -titanium - Ti(N) (140-370 $\mu m).$ Within the first sublayer (TiN) the inclusions of titanium dioxide - TiO $_{\!\! 2}$ phase are evident at the depths up to 25 $\mu m.$ Thorough XRD investigations allowed TiO $_{\!\! 2}$ inclusions also to be detected in depths of 270-370 $\mu m,$ i.e., within the Ti(N) phase contacting with sample core. These "inner" TiO $_{\!\! 2}$ inclusions are obviously remains of

natural passive film spontaneously formed on metal surface just before nitriding. The surface hardness of produced layers was about 1400 HV0.05. The hardness of the as received Ti-1Al-1Mn titanium alloy was about 400 HV0.05.

In Fig. 2(A-D) potentiodynamic polarization curves registered at chosen distances from the initial surface of nitrided Ti alloy are presented. Cathodic plots exhibit Tafel-like character with anomalously big slopes (ca 0.30 to 0.36 V/logi) and with reproducible "hump" at E > -0.7 V. The cathodic hump has a shape of limiting current, however, our additional tests (at stirring rates of 2 - 25 rps) showed that it did not depend on solution agitation. According to the literature [7,15,20], the big slope for cathodic process can be ascribed to formation of TiH, phase on the surface. The cathodic hump disappears at greater distances from the starting surface - apparently, hydride formation is facilitated in the presence of TiN compound. However, in the vicinity of OCP the cathodic slope distinctly decreases and it takes on values of nearly 0.12V, i.e., close to its theoretical value on metallic surfaces. Possibly, the hydride phase transforms into Ti or TiO₂ at potentials $E \approx -0.5$ V.

Fig. 3 presents depth profiles of current densities read from polarization curves at five characteristic potentials: $-1.0~\rm V$ (hydride formation), $-0.75~\rm V$ (hydrogen gas evolution on TiH $_2$), $+0.5~\rm V$ (primary passivation), $+1.6~\rm V$ (oxygen evolution - anodic peak) and $+2.5~\rm V$ (secondary passivation). As shown, nitriding accelerates electrode processes at strongly cathodic ($-1.0~\rm V$) and strongly anodic polarizations ($+2.5~\rm V$). For potentials closer to OCP ($-0.5~\rm to$ $-0.3~\rm V$) the negative role of nitriding on external currents gradually disappears. What is more, at potentials 0.1 to 0.2V more positive than OCP, the strong inhibition of anodic process is clearly visible, especially for depths 0 - 100 μ m (compare polarization curves in Figs. 2A and 2B for $E \approx -0.2~\rm V$).

Fig. 4 shows the reciprocal of polarization resistance $(1/R_0 = \Delta i / \Delta E$ at potential range OCP ± 20 mV) versus the distance from the initial surface of nitrided titanium alloy. As it is known [34], 1/R_n is proportional to the corrosion rate (for corroding material) or to exchange current density (i₀) of simple electrode system (for example, H^+/H_2). Assuming formally $b_3 = \infty$ (passivation) and $b_c = 0.12V$ we get $i_{corr} = 0.052/R_p$ or $i_0 = 0.026/R_p$. It results from Fig. 4 that corrosion rate for the alloy core (> 400 µm) is ca 0.075 mAcm⁻². Within the Ti(N) layer the corrosion process is 2-3 times slower, what is more, for the most outer parts of nitrided layer, owing to efficient passivation of nitride compound layers, we probably register io currents of H+/H2 system (OCP becomes practically equal to $E_{\mathrm{H}^+/\mathrm{H}_2}^{\mathrm{eq}}$). The $\mathrm{TiO_2}$ inclusions present in the outer TiN compound layer seem to inhibit the

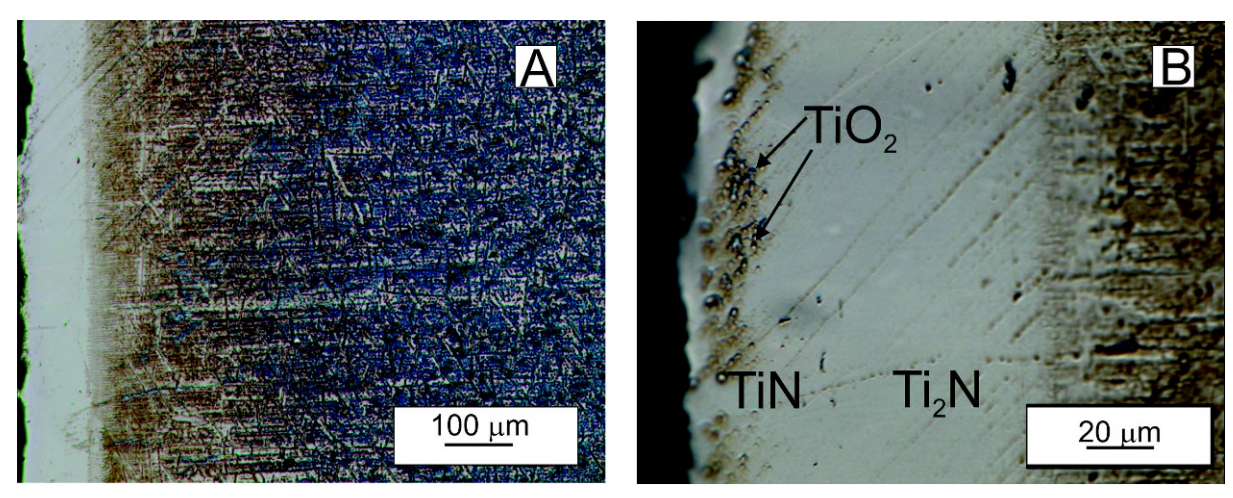


Figure 1. Microstructure of (A) nitride surface layer TiN+Ti₂N+ αTi(N) on Ti-1Al-1Mn titanium alloy and (B) TiN+Ti₂N nitrides layer with TiO₂ precipitations (10-20 μm from the surface).

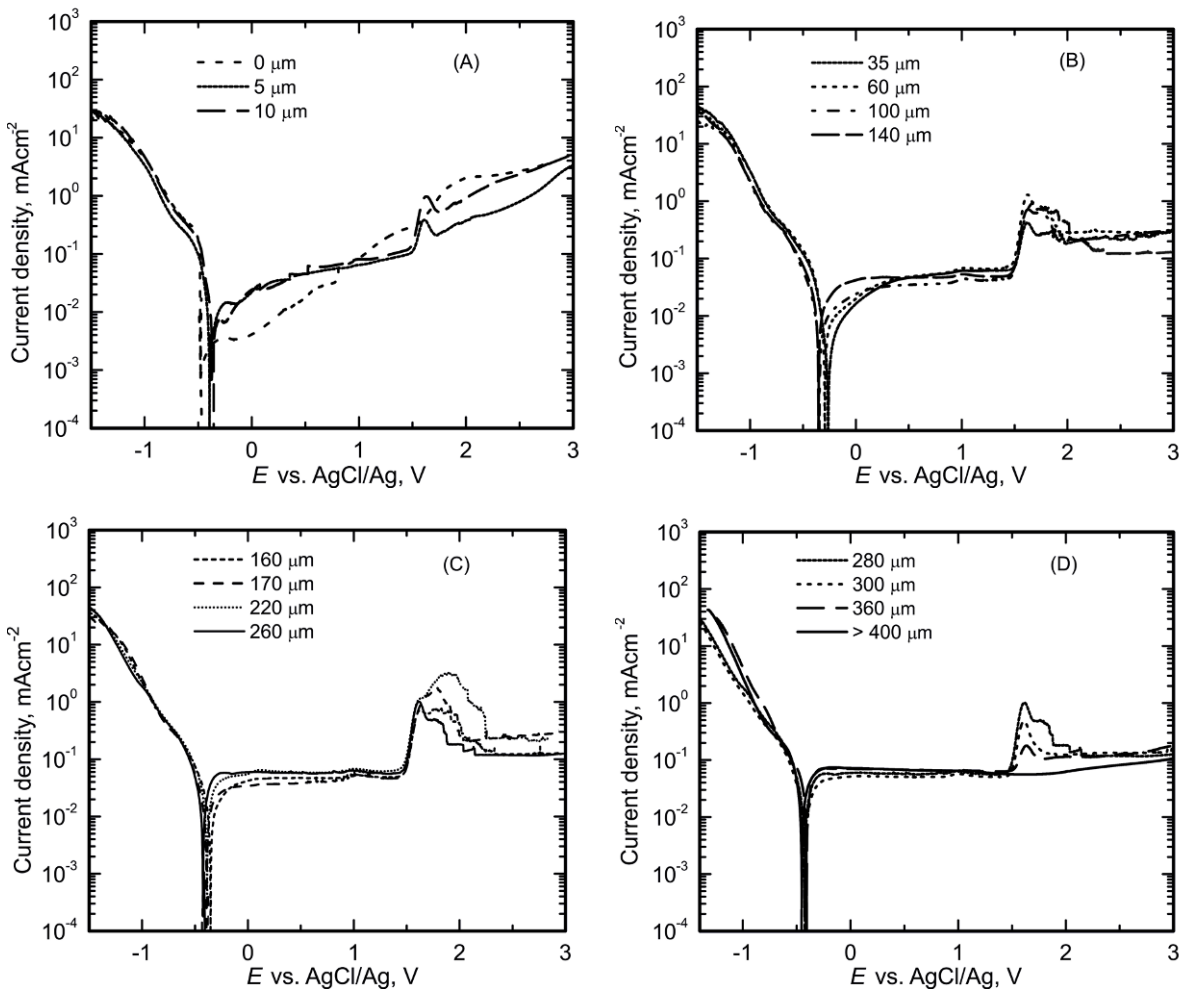


Figure 2. Potentiodynamic polarization curves of glow-discharge nitrided Ti-1Al-1Mn titanium alloy at different depths: (A) external nitrided layer with TiO₂ precipitations, (B) TiN + Ti₂N compound layer, (C) αTi(N) - solid solution and (D) αTi(N)+TiO₂ precipitations. Experimental conditions: 25°C, 0.5 M Na₂SO₄, pH = 2, Ar, stirring rate: 12 rps, potential scan rate: 10 mV s⁻¹.

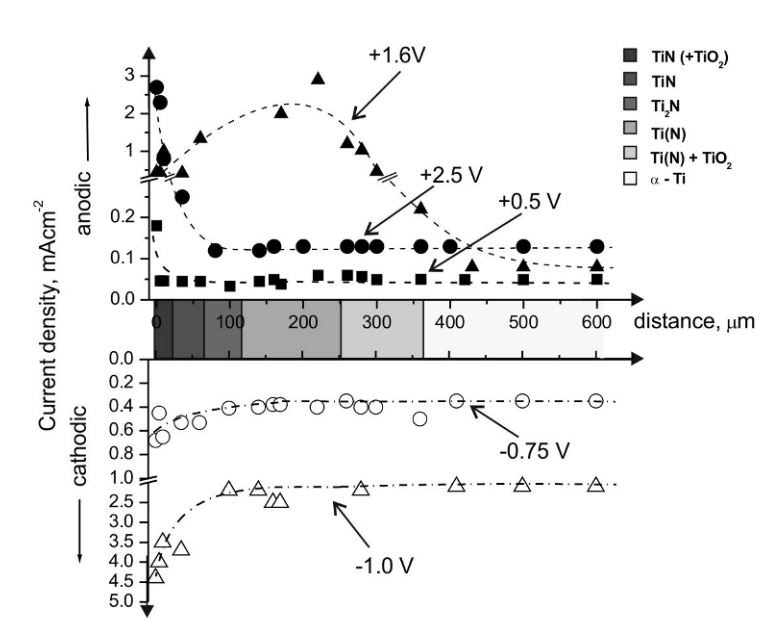


Figure 3. Depth profiles of cathodic- and anodic current densities at characteristic potentials: −1.0 V (hydride formation), −0.75 V (hydrogen evolution on TiH₂), +0.5 V (primary passivation), 1.6 V (oxygen evolution - anodic peak) and +2.5 V (secondary passivation). The current densities were read from potentiodynamic polarization curves (Figs. 2A-2D).

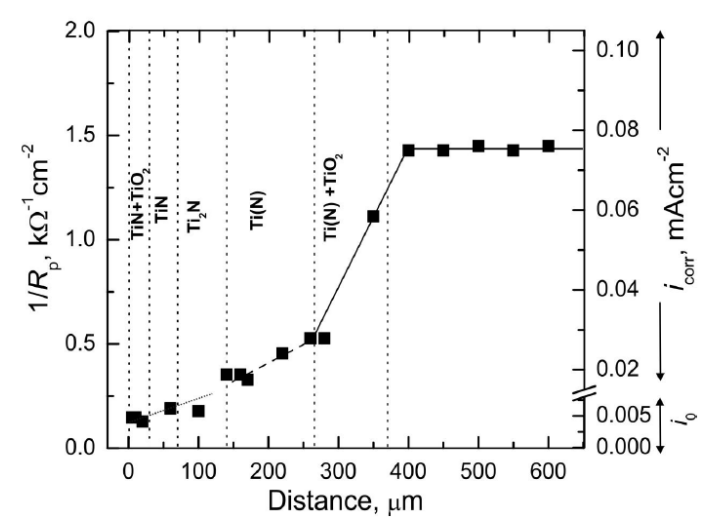


Figure 4. Depth profile of reciprocal of polarisation resistance and corrosion current density (for depths up to 140 mm – exchange current density of H+/H₂ system) of the nitrided Ti-1Al-1Mn titanium alloy in sulphate solution with pH = 2.

electrode processes a little. On the other hand, ${\rm TiO}_2$ precipitates present in Ti(N) solid solution (depths 250 -370 μ m) strongly accelerate the corrosion process. The accuracy of measured $1/R_p$ values is very good for relatively big corrosion rates (0.05 - 1 mA cm⁻²). For lower rates of the electrode process we evaluate the scatter of experimental results to be \pm 10%.

At corrosion potentials (ca -0.5 to -0.4 V) at which cathodic/anodic transition takes place (e.g. Fig. 2C) the Ti nitrided surface gradually passivates (Ti-N species oxidize to TiO₂, possibly with formation of oxynitrides

and elemental nitrogen [4]). In certain simplification the partial electrode processes at potentials close to OCP most probably proceed in the following ways:

Cathodic reactions:

Ti + 2H⁺ + 2e
$$\rightarrow$$
 TiH_{2(s)}
 $E_{(pH=2)}^{eq}$ = -0.32V (vs AgCl/Ag) (1a)

$$4H^+ + 4e \rightarrow 2H_{2(g)}$$

 $E_{(pH=2)}^{eq} = -0.34V (vs AgCI/Ag)$ (1b)

Anodic reaction:

$$TiH_{2(s)} + 2H_2O - 6e \rightarrow TiO_{2(s)} + 6H^+$$

 $E_{(pH=2)}^{eq} = -0.83V \text{ (vs AgCI/Ag)}$ (2)

Thus, the overall reaction of corrosion process should occur at corrosion potential located within -0.32 to -0.83 V range :

$$Ti + 2H_2O \rightarrow TiO_{2(s)} + 2H_{2(g)}$$

 $E_{corr} = -0.83 \text{ to } -0.32V \text{ (vs AgCl/Ag)}$ (3)

It is worth noting that for the most outer layers (up to 10 µm) the anodic currents are comparatively low and increase with further anodic polarization. This way, it should be assumed that nitride phases effectively inhibit the partial anodic reaction (Reaction 2). For the most outer TiN layers the anodic currents, directly above OCP, are 0.003 to 0.01 mA cm⁻², i.e., ca an order of magnitude lower than these for the depths of > 100 µm (compare Figs. 2A and 2B). On the other hand, for depths > 140-260 µm, directly above OCP, the anodic currents take on practically constant values, on the level of 0.05 mA cm⁻² - evidently the Ti(N) solid solution does not inhibit the anodic process (Reaction 2). There is a very important observation relating the measured value of OCP potential: at the depths up to 140 µm (Figs. 2A) and 2B) the OCP is -0.4 to -0.3 V, i.e., it corresponds to equilibrium potentials of Reactions 1a and 1b. As it results from fundamentals of electrochemistry, the equilibrium potential of H+/H2 system should always be more negative than the corrosion potential of metal corroding with hydrogen depolarization. This way, it is reasonable to assume that the OCP potential found for the depths up to 140 µm describes the H⁺/H₂ equilibrium, similarly as it was observed for other easily passivating metals, including AISI 316L stainless steel (in acetic acid, pH = 2) [35].

For nitrided Ti-alloy, the potential range between $E_{\rm corr}$ and 1.5 V corresponds to primary passivation with formation of TiO₂ phase, so the TiN or Ti(N) zones are being gradually enriched with TiO₂ (formation of oxynitride phase [4,14]).

At potential > +1.5 V a distinct increase of anodic process rate is visible for nitrated layers and the anodic peak is the highest for the depths of 200 μm (solid solution of atomic nitrogen in titanium). For greater depths, the height of anodic peak gradually decreases and for the alloy core it completely disappears. Thermodynamic analysis shows that the observed peak corresponds to oxygen evolution (2H₂O −4e→

 $O_2 + 4H^+$ for which $E_{(pH=2)}^{eq} = +0.89 \text{ V } vs \text{ AgCl/Ag}$). The left side slope of the peak is 0.12 V, i.e., typical for O, evolution reaction appropriately to Krasilshchikov mechanism [36,37]. The oxygen evolution overpotential $(\eta_{\rm O_2})$ on nitrided Ti surface is ca 0.6 V, although, as it is known from literature [38], after its full oxidation the η_{o} is much greater (even up to 10 V), owing to definitely dielectric properties of TiO2. As it results from Fig. 2 (B-D), oxygen (or other water oxidation intermediates) produced on the nitrided surface evidently react with nitrogen containing titanium, Ti-N species are gradually transferred into TiO2 and oxygen evolution vanishes. At potentials 1.8 - 2.0 V secondary passivation begins on nitrided titanium and anodic currents in the secondary passivation region are 2-5 times greater than these in the region of primary passivation. According to Lavrenko et al. [14], the final oxidation of Ti-N species to TiO₂ occurs at potentials > 1.7 V which is in good compliance with our research. The TiO, phases formed as the result of Ti-N oxidation are presumably less compact and more porous than TiO, formed on pure titanium and, thus, anodic currents in secondary passivation region are noticeably greater for the depths of < 100 µm compared to the alloy core.

4. Conclusions

- Thin outer layers (up to 25 µm) of nitrided titanium alloy, built of titanium nitride-TiN containing TiO_2 inclusions, show nearly an order of magnitude lower electrode process rates than the inner zones $(\text{TiN+Ti}_2\text{N} \text{ and } \alpha \text{Ti(N)})$ and are 20-30 times lower than corrosion current of the alloy core.
- ${\rm TiO_2}$ precipitates present in the TiN outer layers effectively inhibit the partial electrode (mainly anodic) processes. On the other hand, the ${\rm TiO_2}$ precipitates clearly accelerate the corrosion of inner ${\rm \alpha Ti}(N)$ solid solution phase
- Acid corrosion process of titanium- and nitrided titanium alloy includes ${\rm TiH_2}$ formation in cathodic region which manifests itself with anomalously high slope (> 0.3 V/log*i*) of cathodic Tafel lines.
- For nitrided titanium alloy, unlike for alloy core, anodic peaks at $E \approx 1.6$ V appear owing to relatively small oxygen evolution overpotential on nitrided phases
- The anodic peak divides the passive range into primary- and secondary passivation regions for nitrided Ti-alloy. In primary passivation region the oxynitride phases most probably exist on the Ti surface; in secondary passivation region oxynitrides oxidize to TiO₂.

References

- [1] P.M. Perillo, Corrosion 62, 182 (2006)
- [2] D. Starosvetsky, I. Gotman, Biomaterials 22, 1853 (2001)
- [3] A. Pankiew, W. Bunjongpru, N. Somwang, S. Porntheeraphat, S. Sopitpan, J. Nukaew, C. Hruanun, A. Poyai, J. Microsc. Soc.-Thailand 24 (2), 103 (2010)
- [4] J. Piippo, B. Elsener, H. Bohni, Surf. Coat. Tech. 61, 43 (1993)
- [5] B.N. Arzamasov, L.G. Kirichenko, A.N. Kuznetsov, T.V. Soloveva, Met. Sci. Heat Treat. 40, 378 (1998)
- [6] S. Szmukler-Moncler, M. Bischof, R. Nedir, M. Ermrich, Chin, Oral Impl. Res. 21, 944 (2010)
- [7] K. Videm, S. Lamolle, M. Monjo, J.E. Ellingsen, S.P. Lyngatadaas, H.J. Haugen, Appl.Suf. Sci. 255, 3011 (2008)
- [8] A. Zhecheva, W. Sha, S. Malinov, A. Long, Surf. Coat. Tech. 200, 2192 (2005)
- [9] H.J. Goldschmidt, Interstitial Alloys (Butterworths, London, 1967)
- [10] S. Malinov, A. Zhecheva, W. Sha, Proc. 13th IFHTSE Congress (ASM International, Materials Park, OH, 2003) 344
- [11] A. Czyrska-Filemonowicz, P.A. Buffat, M. Lucki, T. Moskalewicz, W. Rakowski, J. Lekki, T. Wierzchon, Acta Mater. 53(16), 4367 (2005)
- [12] E. Czarnowska, M. Ossowski, J. Morgiel, T. Wierzchon, J. Nanosci. Nanotechnol. 11, 8917 (2011)
- [13] T.P. Hoar, Platinum Met. Rev. 4, 59 (1960)
- [14] V.A. Lavrenko, V.A. Shvets, N.V. Boshitskaya, G.N. Makarenko, Powder Metal. Met. Ceram. 40, 630 (2001)
- [15] A.I. Shcherbakov, Zashchita Met. 38, 174 (2002) (in Russian)
- [16] M.C. Burrell, N.R. Armstrong, Langmuir 2, 37 (1986)
- [17] I. Gurappa, Mater. Charact. 51, 131 (2003)
- [18] M.J. Donachie, Jr., Titanium A Technical Guide, 2nd edition (ASM International, Materials Park, USA, 2000)
- [19] M.J. Munoz-Portero, J. Garcia-Anton, J.L. Guinon, R. Leiva Garcia, Corros. Sci. 53, 1440 (2011)
- [20] A.I. Shcherbakov, I.V. Kasatkina, Zashchita Met. 37, 435 (2001) (in Russian)

- [21] M.S. Khoma, O.M. Romaniv, O.I. Kuntyi, A.I. Tymchyshyn, Mater. Sci. 36, 780 (2000)
- [22] R. Karpagavalli, A. Zhou, P. Chellamuthu, K. Nguyen, J. Biomed. Mater. Res., Part A 83A, 1087 (2007)
- [23] L.H. Li, Y.M. Kong, H.W. Kim, Y.W. Kim, H.E. Kim, S.J. Heo, J.Y. Koak, Biomaterials 25, 2867 (2004)
- [24] H.W. Kim, Y.H. Koh, L.H. Li, S. Lee, H.E. Kim, Biomaterials 25, 2533 (2004)
- [25] W. Han, Y. Wang, Y. Zheng, Adv. Mater. Res. 79-82, 389 (2009)
- [26] R. Carbone, I. Marangi, A. Zanardi, L. Giorgetti, E. Chierici, G. Berlanda, A. Podestà, F. Fiorentini, G. Bongiorno, P. Piseri, P.G. Pelicci, P. Milani, Biomaterials 27, 3221 (2006)
- [27] W. Wilhelmsen, A.P. Grande, Electrochim. Acta 35, 1913 (1990)
- [28] A. Rauscher, Z. Lukacs, Mater. Corros. 39, 280 (1988)
- [29] Z.A. Foroulis, Mater. Corros. 30, 477 (1979)
- [30] (a) M. Stern, H. Wissenberg, J. Electrochem. Soc. 106, 755 (1959); (b) M. Stern, H. Wissenberg, J. Electrochem. Soc. 106, 759 (1959)
- [31] K. Jagielska-Wiaderek, H. Bala, P. Wieczorek, J. Rudnicki, D. Klimecka-Tatar, Arch. Metall. Mater. 54, 115 (2009)
- [32] K. Jagielska-Wiaderek, H. Bala, P. Wieczorek, J. Rudnicki, Arch. Metall. Mater. 55, 515 (2010)
- [33] K. Jagielska-Wiaderek, Arch. Metall. Mater. 57, 646 (2012)
- [34] Shreir's Corrosion, Electrochemical Methods, 4th edition (Elsevier, UK, 2010) Vol. 2, 1358
- [35] H. Bala, L. Adamczyk, E. Owczarek, T. Gruetzner, B.Ch. Seyfang, Ochr. przed Korozja 55, 460 (2012) (in Polish)
- [36] A.N. Krasilshchikov, Zh. Fiz. Khim. 37, 531 (1963) (in Russian)
- [37] M.E. Lyons, R.L. Doyle, M.P. Brandon. Phys. Chem. Chem. Phys. 13(48), 21530 (2011)
- [38] Shreir's Corrosion, Corrosion of Titanium and its Alloys, 4th edition (Elsevier, UK, 2010) Vol. 3, 2042